Brain Connectomics in Early Adolescence Predict Suicidal Ideation Severity in Later Adolescence

Jaclyn S. Kirshenbaum, BA[1*], Rajpreet Chahal, PhD[1], Tiffany C. Ho, PhD[2], Lucy S. King, BA[1], Anthony J. Gifuni, MD[1,3], Dana Mastrovito, PhD[1], Saché M. Coury, BA[1], Rachel L. Weisenburger, BS, BA[1], and Ian H. Gotlib, PhD[1]

[1] Department of Psychology, Stanford University, 450 Jane Stanford Way, Stanford, CA, USA

[2] Department of Psychiatry, University of California, San Francisco, CA, USA

[3] Psychiatry Department and Douglas Mental Health University Institute, McGill University, Montréal, Québec, Canada

*Corresponding author: Jaclyn S. Kirshenbaum, Department of Psychology, Building 420, Jordan Hall, Stanford University, Stanford, California 94305; E-mail jschwar2@stanford.edu

Abstract: 251 words

Article Body: 5416 words

Figures: 2

Tables: 4

Supplemental Information: 1

Supplemental Figures: 1

Supplemental Tables: 4

Abstract

Suicidal ideation (SI) typically emerges during adolescence but is challenging to predict. Given the consequences of SI, it is important to identify neurobiological and psychological predictors of SI in adolescents in order to improve suicide prevention strategies. We used graph theoretical methods to examine whether, and which, local properties of functional brain topology in early adolescence can predict severity of subsequent SI. In 109 participants (61 female) ages 9-13 years, we assessed clinical and participant characteristics and obtained resting-state fMRI data (baseline). We examined inter-regional functional connectedness across 250 brain regions by computing measures of nodal interconnectedness: local efficiency, eigenvector centrality, nodal degree, within-module z-score, and participation coefficient. A LASSO regression identified a linear combination of the most important predictors of SI severity measured approximately 4 years later. The LASSO analysis identified a combination of 8 predictors of future SI severity (R^2=.23) including internalizing symptom severity as the largest predictor (β=.13). The remaining predictors were brain-based including nodal degree of the inferior frontal gyrus (β=-.08), precentral gyrus (β=-.07), fusiform gyrus (β=.05), and inferior temporal gyrus (β=.03), within-module degree of the substantia nigra (β=.06) and inferior parietal lobe (β=-.03), and eigenvector centrality of the subgenual cingulate gyrus (β=.03). Our findings suggest that along with early symptoms of internalizing behaviors, network properties of the brain in early adolescence, a period when SI may not be clinically evident, are markers of vulnerability for SI severity later in adolescence. Research is needed to validate the clinical utility of these markers as predictors of suicidal thoughts.

Introduction

Suicide is the second-leading cause of death in adolescents, resulting in approximately 5,000 adolescent deaths annually (National Center for Health Statistics (NCHS), National Vital Statistics System, National Center for Injury Prevention and Control, Centers for Disease Control and Prevention, & National Institute of Mental Health (NIMH), 2017). Further, suicide rates among individuals ages 10-19 years have increased dramatically over the past decade in the United States (Ruch et al., 2019). Unfortunately, given their high heterogeneity, suicidal thoughts and behaviors (STBs) are difficult to characterize and predict. In individuals with psychiatric symptoms, hopelessness and prior STBs are relatively strong indicators of future suicidal thoughts (Franklin et al., 2017). Certainly, it is important to study individuals who already have clinically relevant risk factors, such as mood disorders; however, suicidal ideation (SI) is prevalent in nonclinical and subclinical samples of community youth. Because many community youth do not seek help for their suicidal thoughts, SI can go undetected (Hawton, Saunders, & O'Connor, 2012). Therefore, it is important that we identify factors that predict suicidal thoughts in non-clinical samples of individuals before more severe suicidal behaviors emerge.

Biologically-based characteristics may add important information to the prediction of STBs in non- and subclinical youth. In this context, investigators have begun to assess neural factors that are associated with STBs in adolescents (Auerbach, Pagliaccio, Allison, Alqueza, & Alonso, 2020; Gifuni et al., 2020; Schmaal et al., 2020; Whalen, Luby, & Barch, 2018). SI is an important precursor to suicidal behaviors (Brent et al., 2009; Klonsky, May, & Saffer, 2016; Prinstein et al., 2008). Although the literature examining neural correlates of SI in adolescents has grown over the past several years, it is still much sparser than is the literature with adults. Nevertheless, several studies have used resting-state functional magnetic imaging (rs-fMRI) to characterize STBs in depressed youth. For instance, greater STBs are associated with higher connectivity between the precuneus of the default mode network (DMN) – a network of regions

consistently related to self-referential processing, including rumination (Menon, 2011) – and superior frontal gyri, but with lower connectivity between the posterior cingulate cortex of the DMN and a cluster including the lateral occipital cortex and fusiform gyrus (Schreiner, Klimes-Dougan, & Cullen, 2019). In addition, lower functional connectivity *within* the DMN, the executive control network (ECN) – regions associated with inhibitory control and decision-making (Cao et al., 2020; Menon, 2011; Uddin, 2015), and the salience network (SN) – regions that respond to emotionally salient stimuli (Seeley et al., 2007) – are associated with greater lifetime SI (Ordaz, Goyer, Ho, Singh, & Gotlib, 2018). Importantly, these findings suggest that disruptions in functional connections are widely distributed.

The studies reviewed above have used either seed-based analysis or whole-brain Independent Component Analysis (ICA) to elucidate which networks are associated with SI. Another approach to examining whole-brain connectivity patterns involves the use of graph theoretical methods, in which the brain is represented as a network (i.e., graph) composed of nodes (brain regions) and edges (connections) (Sporns, 2018). Using this framework, researchers are able to characterize the functional and structural organization of the whole brain on both global (network-wide) and local (nodal) levels (Rubinov & Sporns, 2010). Particularly with functional networks, graph theory allows investigators to measure functional relations between nodes, even if they do not share direct anatomical projections (Zhang, Braun, Tost, & Bassett, 2020). The whole-brain graph theoretical approach allows researchers to quantify important information about the organizational properties of specific regions in the context of the overall brain network, which may be informative for identifying large-scale and local disruptions in network functioning that are associated with STBs.

Few studies have used graph theory to examine the functional neural architecture underlying SI and related behaviors, and no studies have yet used this approach with adolescents. Studies using graph theory with rs-fMRI have typically focused on differences between depressed adults with and without histories of suicide attempt (Weng et al., 2019), and

among ideating adults with and without previous attempts and non-ideating adults with depression (Kim et al., 2017). These studies have found that connections of the thalamus and superior frontal gyrus (SFG) with the rest of the brain are associated with severity of SI. Further, in examining the possible link between a family history of attempt and current STBs, Wagner et al. (2019) suggested that suicidal behavior is associated with heritable impairments in global brain functioning, characterized by weaker connections among nodes across the brain, and by reduced functional connectivity of the ventral and dorsal PFC (Schmaal et al., 2020; Wagner et al., 2019).

Research examining the graph theoretical functional correlates of STBs offers important insights concerning neural alterations in individuals who engage in these harmful thoughts and behaviors. These studies have primarily included individuals with a history of attempt, current and/or past ideation, or diagnoses of a mood disorder. Because these studies are generally cross-sectional, however, it is not clear whether these factors can *predict the subsequent severity* of these suicide-related difficulties. There is an urgent need to identify neurobiological factors early in adolescence, when SI is less prevalent, that prospectively relate to severity of suicidal thoughts in order to guide the development of novel preventative techniques aimed at reducing the most devastating sequela of STBs: suicide attempts.

Suicide attempts are rare, but the consequences are dire. Machine learning (ML) has therefore gained traction because of the potential to have high impact in increasing sensitivity to identify imminent suicidal behaviors (Cox, Moscardini, Cohen, & Tucker, 2020). STBs appear across mental health disorders, which is one reason why STBs are so difficult to predict. One advantage of ML is the ability to search a large set of models and then pick the one that increases model performance, which can thus yield more precision in characterizing the variability in psychopathology (Bzdok & Meyer-Lindenberg, 2018). There are several challenges that come with a method that aims to increase predictive accuracy on datasets with a large number of variables without a strong theoretical basis (Cox et al., 2020). One challenge is interpretation of the output –

the independent variables that are considered important predictors of STBs. Specifically, it can be challenging to interpret the clinical significance of each variable that is considered "important" within a particular dataset because more often than not they are not based on pre-specified hypotheses or theory (Cox et al., 2020). Given the nascent stage of biological predictors of STBs, we aimed to use both hypothesis-driven and data-driven approaches to characterize organizational properties of the whole brain in concert with psychological and environmental factors that previous research have shown to be important to identify the combination of factors that predict future severity of SI.

The goal of the present study was to use graph theoretical methods to identify whether, and which, local properties of functional brain organization in early adolescence (ages 9-13) with other participant characteristics to predict the severity of self-reported SI in later adolescence (approximately 4 years later; ages 13-17). We examined the functional interconnectedness of each brain region with the rest of the brain using the metrics local efficiency, eigenvector centrality, nodal degree, within-module z-score, and participation coefficient. Although graph theory analyses involve data-driven exploration, based on the studies described above we hypothesized that internalizing severity, early life stress severity, and nodal properties of subcortical, frontal, cingulate, and insular structures will predict the severity of later SI.

Methods and Materials

Participant Recruitment

We recruited 214 males and females (121 females) ages 9-13 years (*M*=11.38, *SD*=1.05) from the community to participate in a longitudinal study assessing the effects of early life stress (ELS) on neurobiological development over puberty. Because participants were matched on pubertal status, males were older than females. Participants were recruited from the San Francisco Bay Area through print and online advertisements, unselected for psychiatric disorders or suicidality history. Exclusion criteria included contraindications for MRI scan (e.g., metal implants, braces), history of major neurological disorder, intellectual delay, and non-fluent English speakers. For the current study, participants were excluded if they did not complete a

functional resting-state scan at baseline or withdrew from the study (N=25) or if their functional scan data included excessive signal dropout (N=8) or movement defined by 20% of volumes>2 SD above mean framewise displacement (N=8), resulting in 174 participants (101 females). At a follow-up session approximately 3-5 years post-baseline, 133 participants were assessed for severity of SI, 17 of whom did not have usable scan data from baseline and 7 of whom we excluded from this analysis based on parent and child-reported history of STBs, resulting in a final sample of 109 participants (see Table 1 for participant characteristics and Supplemental Table 1 for table of medications taken at baseline). In accordance with the Declaration of Helsinki, participants and their parents provided informed written assent and consent, respectively. This study was approved by the Stanford University Institutional Review Board and all participants were compensated for their participation.

Clinical Characteristics

K-SADS-PL. The Kiddie-Schedule for Affective Disorders and Schizophrenia Present and Lifetime (K-SADS-PL) is a semi-structured interview used to establish presence of DSM-IV diagnoses (Kaufman et al., 1997). We asked three questions regarding STBs, involving recurrent thoughts about death, experiencing thoughts about ending their own lives, and attempting to end their own lives. These symptoms were rated as “not present,” “subthreshold,” or “threshold.” Trained interviewers administered the K-SADS-PL to children and their parents at both timepoints. For the current study we examined child-reported information of lifetime and current substance/alcohol use and STBs given that these are risk factors for future STBs (C. A. King et al., 2019). As reported in our participants section, we excluded those who reported threshold levels of STBs at baseline. As expected, no participant in this sample endorsed substance or alcohol use at baseline.

Internalizing Symptom Severity. Participants completed the Youth Self Report (YSR (Earls, Brooks-Gunn, Raudenbush, & Sampson, 2007)), a commonly used measure to assess

internalizing symptoms. The YSR was administered at both time points and had high internal consistency at baseline (α=.80) and at follow-up (α=.82).

Suicidal Ideation. To assess dimensionality of the severity of SI, participants completed the Suicidal Ideation Questionnaire – Junior Form (SIQ-JR; Reynolds, 1988), a 15-item self-report measure of suicidal thoughts in the past month. Scores range from 0-90, with higher scores indicating greater severity. The SIQ was administered at the follow-up assessment and had high internal consistency (Cronbach's α=.97).

Participant Characteristics

Early Life Stress (ELS). To assess history of ELS, adolescents were interviewed at baseline about exposure to different types of stressful experiences using a modified version of the Traumatic Events Screening Inventory for Children (TESI-C; Ribbe, 1996). We calculated an objective severity score, obtained by summing the maximum objective severity scores for each type of stressor endorsed by each adolescent; this method ensured that frequent but less severe events would not be overly weighted (L. S. King et al., 2017). We also calculated a stress sensitivity score that represents participants' cumulative subjective stress severity accounting for cumulative objective stress severity (Ho et al., 2017). See *Supplement* for information about the ELS coding system.

Pubertal Status. To assess pubertal status, participants rated their developmental stage using the Tanner Staging questionnaire (Marshall & Tanner, 1969, 1970; Morris & Udry, 1980) at both baseline and follow up. This questionnaire measures developmental status based on schematic drawings of secondary sex characteristics (pubic hair and breast development for females, pubic hair and testicular development for males) on a scale from 1 (no pubertal development) to 5 (adult level of pubertal development). Within each time point, we averaged the two ratings of the secondary sex characteristics to yield a composite measure of the participants' pubertal status. Self-reported Tanner staging is correlated with physicians' physical examinations of pubertal development (Coleman & Coleman, 2002; Shirtcliff, Dahl, & Pollak,

2009), and with pubertal hormones in this sample (L. S. King, Graber, Colich, & Gotlib, 2020). No participant endorsed taking hormonal contraception at baseline.

fMRI Acquisition and Preprocessing

MRI scans were conducted on a GE Discovery MR750 scanner (GE Medical Systems, Milwaukee, WI) equipped with a 32-channel head coil (Nova Medical). We collected spoiled gradient echo (SPGR) T1-weighted sagittal anatomical images (repetition time [TR]=6.24ms; echo time [TE]=2.34 ms; flip angle=12°; FOV=230 mm; voxel size=0.8984 x 0.8984 x 0.9000 mm; scan time=5:15) to be used for alignment and registration of functional images and for segmenting tissue types for facilitating resting-state fMRI preprocessing. Resting-state BOLD fMRI data were acquired using aT2*-weighted echo planar imaging sequence with 37 axial slices (180 volumes, repetition time [TR]= 2.0 s; echo time [TE]=30 ms; flip angle=77°; FOV=224 mm; voxel size=3.2 mm^3, total scan time=6:00). During the resting-state fMRI scan, participants were instructed to keep their eyes closed but remain awake. After the scan, we ask participants whether they experienced sleepiness during the scan. Results included in this manuscript come from preprocessing performed using *fMRIPrep* 1.5.0 (Esteban et al., 2019); RRID:SCR_016216, which is based on *Nipype* 1.2.2 (K. Gorgolewski et al., 2011; K. J. Gorgolewski et al., 2017); RRID:SCR_002502. See *Supplement* for information on fMRI preprocessing.

Network Construction

Parcellation. Hallquist and Hillary (2018) recommend using an atlas consisting of at least 200 regions of interest (ROIs) (Hallquist & Hillary, 2018). We parcellated each participant's preprocessed structural data into 246 ROIs using the Brainnetome Atlas (L. Fan et al., 2016) plus 4 additional subregions of the basal ganglia (Keuken & Forstmann, 2015). We Fisher-z transformed the Pearson's correlation coefficients of time-series of all pairs of regions to define the edges of the brain network, yielding a 250x250 fully connected, undirected, and weighted graph for each participant.

Defining edges. All negative weights in participants' correlation matrices were set to zero to aid interpretation (Lydon-Staley, Ciric, Satterthwaite, & Bassett, 2018). One challenge in graph theoretical studies is choosing a threshold to determine what constitutes a "connection" from a continuous measure of functional connectivity (i.e., the Pearson's correlation coefficient value) (Hallquist & Hillary, 2018). There is no consensus about how to threshold functional connectivity values, and most recommendations apply to case-control studies (Hallquist & Hillary, 2018). Consequently, we calculated graph metrics over a range of relative density thresholds (Matthews & Fair, 2015) from .10 to .20 in steps of .02. For each graph metric for each of the 250 ROIs, we summed the averages across each pair of thresholds to yield a composite threshold value (van den Heuvel et al., 2017; Hosseini, Hoeft, & Kesler, 2012).

Computation of graph metrics. All graph metrics were calculated based on each participant's weighted correlation matrices using *GraphVar version 2.02* (Kruschwitz, List, Waller, Rubinov, & Walter, 2015), which uses functions from the *Brain Connectivity Toolbox* (BCT; Rubinov & Sporns, 2010). We calculated five local graph metrics per node: local efficiency, eigenvector centrality, nodal degree, within-module z-score, participation coefficient (see Table 2 for definitions), yielding 1250 graph-based predictors. We used *R version 3.6.2* (R Core Team, 2019) for all subsequent statistical analyses. See https://github.com/jackie-schwartz/brain_connect_and_si for code availability.

Relating rs-fMRI graph-based metrics to suicidal ideation

Response Data Distribution and Predictors

Participants scored between 0-70 on the SIQ (*M*=9.09, *SD*=12.99), with an expected low modal response of 2. Because these data were positively skewed (12.84% endorsed 0), we log-transformed the data, yielding a more normal distribution (see *Supplemental Figure 1*). For our predictor matrix, we imputed missing values for variables that did not have complete cases (see *Supplemental Table 2*) using the Multivariate Imputation by Chained Equations (mice) package (Buuren & Groothuis-Oudshoorn, 2011) in R. This method uses the information from the other

variables to predict and impute missing values. With 1250 brain-based graph metrics obtained at baseline, we also included framewise displacement (i.e., head motion during scan) and the baseline demographic and non-brain variables including age, sex, Tanner score, BMI, internalizing symptom severity, the interval between the time points, objective ELS severity, subjective ELS sensitivity, and parent education level as an indicator of socioeconomic status (SES). Thus, 1259 possible predictors (all standardized) were included in the subsequent regularized regression.

Regularized LASSO Regression

Because we had more predictors than observations and expected collinearity among many of these predictors, we conducted a regularized regression analysis (Zou & Hastie, 2005). Specifically, we used least absolute shrinkage and selection operator (LASSO) regression, which applies the L1 penalty and thereby "shrinks" coefficient estimates of redundant variables to zero in order to identify the features that yield the most predictive model (Tibshirani, 1996). After applying the appropriate penalty, the resulting variables will either have zero or non-zero coefficient values. The linear combination of the variables with non-zero coefficient values yields the model that best explains severity of future SI in our sample.

We used the *glmnet* package (Friedman, Hastie, & Tibshirani, 2010) in *R* to perform the regularized LASSO regression employing a full L1 penalty (i.e., $\alpha=1$) and an expected gaussian distribution. We performed leave-one-out cross-validation (LOOCV) using the *cv.glmnet* function to determine the largest λ (i.e., hyperparameter, regularization value) associated with the least mean-squared error (i.e., "lambda.min"). We used this lambda to obtain a sparse matrix of non-zero coefficients. In order to determine model performance, we computed R^2 based on predicted and observed values. LOOCV is appropriate for smaller sample sizes compared to other cross-validation techniques (e.g., validation set approaches) because the training set consists of almost the full dataset (James, Witten, Hastie, & Tibshirani, 2013). Additionally,

compared to other cross-validation approaches LOOCV produces less bias in the test error (James et al., 2013).

Supplemental Analysis of Non-Brain Variables

Given sex and race are important characteristics in predicting STBs (Adrian, Miller, McCauley, & Stoep, 2016; LaVome Robinson, Droege, Hipwell, Stepp, & Keenan, 2016), and because effects of the other baseline demographic and participant characteristics in the LASSO may go undetected due to high penalization, we conducted separate linear regressions to determine which non-graph theory brain-based baseline variables (sex, race, age, BMI, Tanner score, internalizing symptom severity, the interval between the time points, objective ELS severity, subjective ELS sensitivity, SES, mean framewise displacement, sleepiness during scan) were associated with the severity of SI. Most of the results of the OLS regressions are consistent with the LASSO regression. Results and discussion for this analysis are presented in the Supplement (*Supplemental Analysis of Non-Graph theory Brain-based Baseline Variables and Supplemental Table 3)*.

Analysis using Internalizing Severity as an Outcome

To assess whether we captured predictors of SI specifically or internalizing symptoms more broadly, we conducted analyses with severity of internalizing symptoms as the outcome, re-running the LASSO regression replacing SIQ with YSR at follow-up, and keeping all other variables the same as in the primary analysis.

Results

Participant characteristics are presented in Table 1. At baseline, participants were in early adolescence (Mean Tanner stage= 1.97 ± 0.77) and males were significantly older than females (p=.001*)*. In the follow-up sample four years later in mid-to-later adolescence (Mean Tanner stage=4.24±0.71), males remained older than females (p=.057*)*. We assessed SI severity at follow-up, which is when we would expect SI to develop (Nock et al., 2013).

The LOOCV of the LASSO regression used to predict severity of SI yielded an optimal lambda of .19, which resulted in 8 variables with non-zero coefficients (see Table 3, Figure 1), explaining 22.87% of the variance in severity of SI. The brain-based variables were distributed across the basal ganglia, and frontal, temporal, parietal lobes, and cingulate gyri. The only non-brain-based predictor of SI severity was baseline internalizing symptom severity (β=0.1318), which was positively associated with subsequent severity of SI.

The brain-based metrics that were included in the model predicting higher severity of SI were lower nodal degree in the frontal gyrus – specifically right caudal inferior frontal gyrus (β=-0.0807) and the left caudal precentral gyrus (β=-0.0691), followed by higher within module degree right substantia nigra (β=0.0592) and higher nodal degree in the temporal gyrus – specifically the left medioventral fusiform gyrus (β=0.0522) and the inferior temporal gyrus (β=0.0305). Additional predictors were higher eigenvector centrality of the right subgenual cingulate gyrus (β=0.0279) and lower within-module degree of the rostrodorsal inferior parietal lobe (β=-0.0308). We should note that the beta estimates are small due to the penalization that the LASSO applies, which shrinks the coefficients. In fact, 99.37% of variables had their coefficients reduced to zero. To inspect stability of the coefficient estimates, we computed the zero-order correlations, which revealed consistency in the direction of associations across the zero-order correlations and the LASSO results (see Table 3). Importantly, severity of future SI is not predicted by only one brain region or one demographic characteristic; rather, it is the full predictive model that is the linear combination of all 8 features that achieves R^2=.2287.

The LOOCV of the LASSO regression used to predict internalizing symptom severity yielded an optimal lambda of .20, which resulted in 9 variables with non-zero coefficients (see Table 4, Figure 2). Interestingly, some of our results seem to be capturing SI specifically and other predictors seem to be overlapping with internalizing symptom severity more broadly. Overlapping features included lower nodal degree of the right caudal inferior frontal gyrus (β =-0.0302) and higher severity of internalizing symptoms (β =0.0551). However, associations

between interconnectedness of brain regions and internalizing symptom severity are less widespread as compared to associations between interconnectedness and severity of SI. In particular, there is increased interconnectedness in regions of the temporal gyrus, but reduced interconnectedness in regions of the frontal gyrus. Additionally, more participant characteristics such as sex and age appear to be predictors of future internalizing severity, but not of SI severity. Here, 99.29% of variables had their coefficients reduced to zero. As with our SI analysis, to inspect stability of the coefficient estimates, we computed the zero-order correlations, which revealed consistency in the direction of associations across the zero-order correlations and the LASSO results (see Table 4). These results reveal that severity of future internalizing symptoms predicted by only one brain region or one demographic characteristic; rather, it is the full predictive model that is the linear combination of all 9 features that achieves R^2=.1862.

Discussion

Recent meta-analyses have noted the relatively weak effect sizes of clinical and demographic characteristics, where prior STBs are the strongest predictor of future SI (Franklin et al., 2017); however, these symptoms can go undetected in samples of community youth (Hawton et al., 2012). Primarily, it is important to identify factors that predict thoughts before the first attempt even occurs. Identifying neurobiological predictors of SI may increase the effectiveness of prevention and early-intervention based programs. We examined whether interconnectedness of brain regions, as measured with resting-state fMRI, in an unselected sample of early adolescents predicts the future severity of SI in later adolescence. We also included in the analyses baseline clinical and demographic characteristics to examine which combination of variables best predict future severity of SI. A machine learning approach in this context allowed us to elucidate which theoretically important psychological (internalizing severity), environmental (early life stress), and exploratory brain-based variables (graph metrics computed across the whole brain) work in concert to predict future severity of SI. Several brain-

based graph metrics predicted subsequent severity of SI, including some regions that have been identified as associated with STBs, such as caudal precentral gyrus, inferior frontal gyrus, and midbrain regions (cingulate), and some regions that are not identified as frequently in the suicide literature (substantia nigra; SN).

Because our supplemental analysis using internalizing symptoms as an outcome yielded mostly different results, it is possible that that we are explaining a distinct aspect of SI that is transdiagnostic. Importantly the gyri that were implicated in both internalizing and SI severity revealed the same direction of association – namely, interconnectedness of frontal gyrus regions were negatively associated with future internalizing and SI severity, but interconnectedness of temporal gyrus regions were positively associated with future internalizing and SI severity. It is important to note that our analysis did not identify regions that *have* been implicated in previous studies (see Schmaal et al., 2020 and Auerbach et al., 2020 for reviews). For instance, adults who attempted suicide show increased severity of SI with increased functional connectivity between the amygdala and parahippocampal gyrus (Kang et al., 2017). We did not find evidence of the thalamus as predictor of the future severity of SI. Findings concerning functional connectivity of the thalamus in relation to STBs (Schmaal et al., 2020) have been mixed; individuals with a suicide attempt history have increased connectivity of the thalamus relative to those without an attempt history (Jung et al., 2020); however, using task-based fMRI, Pan et al. (2011) found decreased activity of the right thalamus during high-risk decisions in adolescents who had attempted compared to those who had not attempted suicide (Lisa A. Pan et al., 2011).

In the temporal gyrus, more connections of the right inferior temporal gyrus and of the left fusiform gyrus with the rest of the brain was related to greater severity of SI. Previous research has shown greater resting-state activity in the right superior temporal gyrus in adults with a history of suicide attempts had (T. Fan, Wu, Yao, & Dong, 2013), but reduced connectivity of the left fusiform with the posterior cingulate cortex associated with higher severity

of STBs in depressed adolescents (Schreiner et al., 2019). Further, there was a decrease in activation in the left fusiform when adolescents who had attempted suicide view neutral compared to angry emotional faces (L. A. Pan et al., 2013).

Within the frontal gyrus, we found lower degree in left precentral gyrus in relation to future severity of SI. Studies using PET imaging found that the relative metabolic rate of glucose was lower in the precentral gyri in adults who attempted suicide than in those without suicide attempts (Sublette et al., 2013). In their recent review, Schmaal et al. (2020) suggest that the frontal gyrus, specifically the inferior region, facilitates the transition from suicidal thoughts to behaviors because it is involved in cognitive flexibility and behavioral decision-making (Schmaal et al., 2020); we found here that this structure predicted suicidal thoughts. It is possible, however, that if individuals were followed longitudinally, we might see this region more implicated in behaviors. There may be greater overlap in the different communities of brain regions supporting STBs in early adolescence given the less distributed organization of the brain than is the case later in development (Grayson & Fair, 2017). It is important that future studies examine explicitly and systematically whether different brain regions are associated with STBs across development.

The graph metrics we identified are important in elucidating the organizational properties of functional connectivity previously implicated in SI. In summary, we found here that a lower *number of connections (degree)* of areas in the frontal gyrus and a higher number of connections of areas in the temporal gyrus may contribute to biological risk factors for SI. In addition, a higher number of connections of the substantia nigra with its surrounding regions (within-module degree) was associated with increased severity of suicidal ideation. The substantia nigra is a source of dopamine and has largely been studied in the context of motor (Utter & Basso, 2008) and reward related (Richter, Reinhard, Kraemer, & Gruber, 2020) behavior, but is also a region targeted in deep brain stimulation. In fact, one case study found acute stimulation of this region invoked an acute depressive episode with thoughts of “not

wanting to live" (Blomstedt et al., 2008). In line with our findings, this region's connections within the basal ganglia may also contribute to a biological characterization of SI.

Within the parietal lobe, reduced within-module degree was associated with increased SI, meaning that a lower number of connections of the right inferior parietal lobe with its surrounding regions may be contributing to higher severity of SI. This organizational property of the right inferior parietal lobe may be in line with research showing that individuals with depression, SI, and suicidal plans have reduced regional glucose metabolism in the right inferior parietal lobe compared to those with SI only and healthy controls (van Heeringen, Wu, Vervaet, Vanderhasselt, & Baeken, 2017). More research is needed to understand whether reduced regional glucose metabolism is related to a lower number of connections to its surrounding regions. We also identified a higher eigenvector centrality of the right subgenual cingulate cortex (sgCG) associated with SI, which indicates that this region's connection with other highly connected regions is associated with higher severity of SI. Findings of associations between the sgCG and SI have been mixed. For instance, in individuals with treatment resistant depression, there was no evidence of an association between regional glucose metabolism of the sgCG and SI (Ballard et al., 2015); however, other studies have found that inflammation in this region is higher in individuals with SI compared to those without SI (Holmes et al., 2018). In a recent study examining graph metrics in depressed adolescents, certain organizational properties other than eigenvector centrality of the right sgCG were associated with depression severity (Gabbay et al., 2020). However, we did not find this region as part of the model predicting increased internalizing severity in our sample.

We did not find that ELS severity was related to later severity of SI, which is contrary to other studies' findings of a relation between adversity and STBs in adolescent samples (Stewart et al., 2019). In our sample , childhood stress included bullying, negative self-referential processes (e.g., feelings of worthlessness and low self-esteem), which has been associated with an increased risk for STBs (Cha et al., 2018). We took a continuous approach to the

measurement of ELS in this study, assessing a wide range of experiences, including both relatively normative stressors (e.g., moving, parental divorce) and highly threatening events (e.g., physical abuse, sexual assault); approximately 12% of our sample was exposed to these threatening events (L. S. King, Humphreys, Camacho, & Gotlib, 2019). We may have found effects of ELS if more children had been exposed to highly threatening events.

We should note four limitations of the current study. First, we did not obtain information about family history of STBs. Given previous findings of a significant genetic component predicting suicide attempts (Ruderfer et al., 2019), obtaining family history of STBs may have yielded important information about subsequent severity of SI. Second, the distribution of SI at follow-up was skewed – most participants endorsed low severity of SI. It is possible that a distribution with more severe ideation would have yielded different results; future studies will benefit from including a wider range of SI. Third, we used LOOCV to test the reliability of our results; our findings should be replicated using independent samples for cross-validation. If our results are replicated, it would also be beneficial for future research to integrate neuroimaging findings with other more scalable metrics in order to increase the clinical utility of neuroimaging. Finally, our resting-state scan was 6 minutes long. Although longer scan times can improve the reliability of functional connectivity estimates (Birn et al., 2013; Termenon, Jaillard, Delon-Martin, & Achard, 2016), estimates have been found to be reliable in scans as short as 5 minutes (Andellini, Cannatà, Gazzellini, Bernardi, & Napolitano, 2015; Van Dijk et al., 2010).

Despite these limitations, the present study underscores the importance of examining distributed functional architecture of the brain in early adolescence to predict SI severity in later adolescence, a time when suicidal thoughts may dramatically increase (Nock et al., 2013). A strength of our investigation is that we recruited a sample of children and adolescents with minimal psychiatric histories and were able to identify several neurobiological factors that predicted the subsequent severity of SI. Given that we identified organizational properties of regions that are distributed across the brain, it is important for future work to replicate our data-

driven approach, interrogating regions of the brain that might be missed otherwise. Consistent with our results, previous studies have found that neurobiological markers explain more variance in SI severity than do age of depression onset, severity of depressive and anxious symptoms (Ordaz et al., 2018; Schwartz, Ordaz, Ho, & Gotlib, 2019), and duration of depressive episodes (Schreiner et al., 2019). Combined with these previous studies, our findings are useful for understanding and predicting the severity of suicidal thoughts before more severe suicidal behaviors emerge. Given the challenge of identifying risk for SI in adolescence, it is important to delineate factors that increase this risk. Our results underscore that suicidal thoughts are predicted by a combination of biological and psychological factors. Neuroimaging is useful in identifying biological aspects of suicidal thoughts and, when used with other methods, can provide important complementary information about the development of SI. Finally, although we focused in this study on temporally distal risk factors for suicidal thoughts, gaining a better understanding of how the brain is associated with the transition from suicidal thoughts to behaviors is an important direction for future research.

Tables and Figures (in order)

Table 1. Participant Characteristics (N = 109)

Variable	Mean (SD)	Range
Female (%)	55.96	
Age baseline (years)	11.34 (0.98)	9.11 - 13.81
Age_females	11.08 (1.01)	
Age_males	11.66 (0.84)	
Age follow-up (years)	15.49 (1.09)	13.10 - 17.93
Age_females	15.32 (1.18)	
Age_males	15.71 (0.93)	
Interval between baseline and later assessment (years)	4.08 (0.55)	3.25 - 6.57
Tanner baseline	1.97 (0.77)	1 - 4.5
Tanner follow-up	4.28 (0.71)	1.5 - 5
BMI baseline	18.57 (3.67)	12.54 - 30.78
Race (%)		
White	49.54	
Black/African American	7.34	
Latinx/Hispanic	3.67	
Asian	15.60	
biracial	18.35	
other	5.50	
Stress Severity (objective)	5.82 (4.78)	0 - 22
Subjective Stress Sensitivity	-0.06 (0.52)	-2.21 - 1.60
YSR baseline	10.93 (8.13)	0 - 39
YSR follow-up	14.16 (9.67)	0 - 42
SIQ (raw scores)	9.09 (12.99)	0 - 70
SIQ (log transformed)	1.73 (1.08)	0 - 4.26
Head Motion (FD)	0.12 (0.07)	0.04 - 0.38

YSR = Youth Self Report; SIQ = Suicidal Ideation Questionnaire; FD = Framewise Displacement (mean FD across all frames acquired per subject)

Table 2. Description of Graph Metrics

Metric	**Definition**
local efficiency	Efficiency of node neighborhoods. It is a measure of the interconnectedness of neighboring nodes.
eigenvector centrality	A metric of node “influence” based on the number of edges among nodes and connectedness (strength) of neighboring nodes (Hwang, Hallquist, Luna, 2013). This is a measure of weighted centrality to nodes in the network, based on the assumption that more prominent nodes are linked to many other important nodes (Ballarini et al., 2018).
degree	Number of edges connected to that node
within module degree	Z-score of a node's within-module degree; z-scores > 2.5 denote hub status (Power, Schlaggar, Lessov-Schlaggar, Petersen, 2013)
participation coefficient	Whether a node is a connector hub or a provincial hub is based on its participation coefficient. Connector hubs, which connect nodes between different modules, have high participant coefficients; provincial hubs, which link nodes within the same module, have lower participant coefficients.

Table 3. Predictors of Suicidal Ideation Severity from LASSO Regularized Regression (N=109)

Model	**ROI/Variable**	**x**	**y**	**z**	**Graph Property**	**Coefficient Estimate (β)**	**Zero-order correlations (β)**
LOOCV alpha = 1 lambda = 0.1863286	Internalizing severity at baseline				---	0.1318	0.18
	caudIFG (R)	54	24	12	Degree	-0.0807	-0.28
	caudvlPrG (L)	-49	5	30	Degree	-0.0691	-0.15
	SN (R)	8	-14	-14	Within-module degree	0.0592	0.21
	medventFuG (L)	-31	-64	-14	Degree	0.0522	0.23
	intlatITG (L)	-56	-58	4	Degree	0.0305	0.18
	sgCG (R)	5	41	6	Eigenvector centrality	0.0279	0.14
	rostdorIPL (R)	47	-35	45	Within-module degree	-0.0308	-0.07

Note. Model R^2= 0.2287. Predictors are listed in order of the magnitude of their coefficient estimates for each Model. ROI = region of interest; LASSO = least absolute shrinkage and selection operator; CV = cross-validation; caudIFG = caudal inferior frontal gyrus; caudvlPrG = caudal ventrolateral precentral gyrus; SN = substantia nigra; medventFuG = medioventral fusiform gyrus; intlatITG = intermediate lateral inferior temporal gyrus; sgCG = subgenual cingulate gyrus; rostdorIPL = rostrodorsal inferior parietal lobe

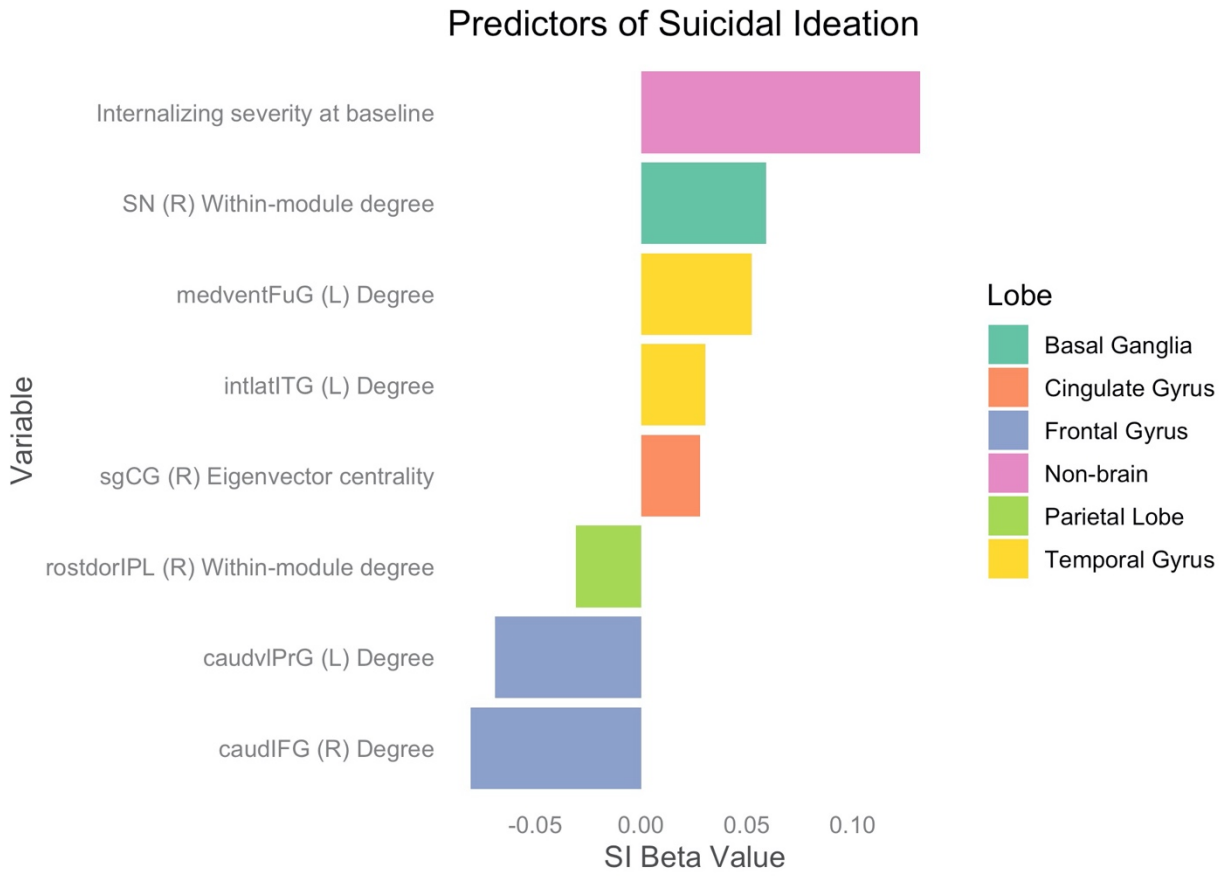

Figure 1. Predictors of Suicidal Ideation. caudIFG = caudal inferior frontal gyrus; caudvlPrG = caudal ventrolateral precentral gyrus; SN = substantia nigra; medventFuG = medioventral fusiform gyrus; intlatITG = intermediate lateral inferior temporal gyrus; sgCG = subgenual cingulate gyrus; rostdorIPL = rostrodorsal inferior parietal lobe

Table 4. Predictors of Internalizing Symptom Severity from LASSO Regularized Regression (N=109)

Model	**ROI/Variable**	**x**	**y**	**z**	**Graph Property**	**Coefficient Estimate (β)**	**Zero-order correlations**
LOOCV	intlatITG (L)	-56	-58	4	Eigenvector centrality	0.1195	0.32
alpha = 1	Sex				---	0.0759	0.57
lambda = 0.201221	medventFuG (R)	31	-62	-14	Degree	0.0678	0.26
	Internalizing severity at baseline				**---**	**0.0551**	**0.29**
	Age at baseline				---	-0.0532	-0.27
	caudIFG (R)	**54**	**24**	**12**	**Degree**	**-0.0302**	**-0.28**
	caudPhG (L)	-25	-25	-26	Local efficiency	0.0130	0.23
	vIFG (L)	-52	13	6	Eigenvector centrality	-0.0107	-0.25
	orbOrG (R)	40	39	-14	Participation coefficient	-0.0073	-0.23

Note. Model R-squared = 0.1861916. Predictors are listed in order of the magnitude of their coefficient estimates for each Model. Bolded variables indicate overlap with predictors of suicidal ideation. ROI = region of interest; LASSO = least absolute shrinkage and selection operator; CV = cross-validation; intlatITG = intermediate lateral inferior temporal gyrus; medventFuG = medioventral fusiform gyrus; caudIFG = caudal inferior frontal gyrus; caudPhG = caudal parahippocampal gyrus; vIFG = ventral inferior frontal gyrus; orbOrG = orbital area 12/47

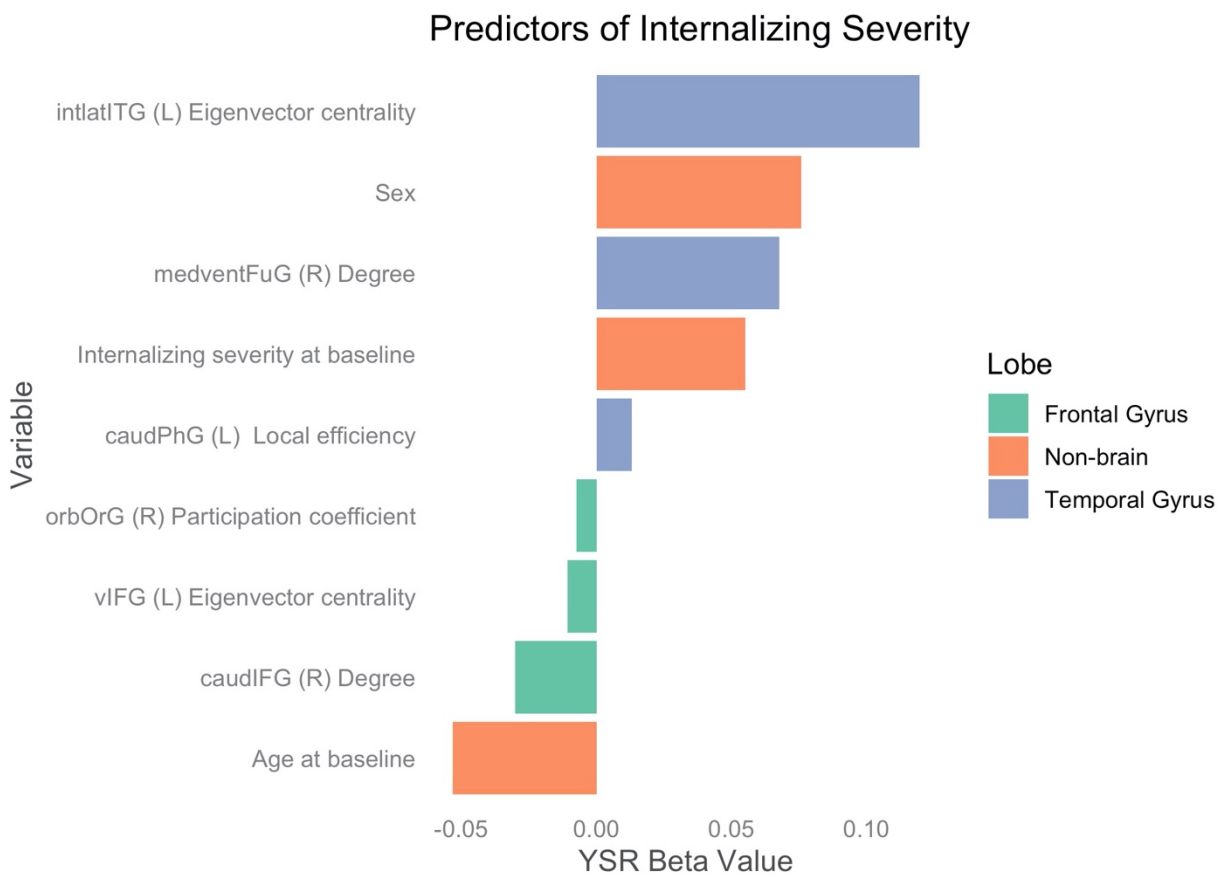

Figure 2. Predictors of internalizing symptom severity. intlatITG = intermediate lateral inferior temporal gyrus; medventFuG = medioventral fusiform gyrus; caudIFG = caudal inferior frontal gyrus; caudPhG = caudal parahippocampal gyrus; vIFG = ventral inferior frontal gyrus; orbOrG = orbital area 12/47

Funding and Disclosure

This research was supported by the National Sciences Foundation (Graduate Research Fellowship to JSK and LSK), National Institutes of Health (NIH; R37MH101495 to IHG, F32MH120975 to RC, K01MH117442 to TCH), the Stanford University Precision Health and Integrated Diagnostics Center (PHIND to IHG, TCH, and JSK) and the Fonds de Recherche du Québec – Santé (FRQS/MSSS Resident Physician Health Research Career Training Program to AJG). The content is solely the responsibility of the authors and does not necessarily represent the official views of the NIH. All authors report no financial interests or potential conflicts of interest. The funding agencies played no role in the design and conduct of the study; collection, management, analysis, and interpretation of the data; and preparation, review, or approval of the manuscript.

Acknowledgments

We thank Michelle Sanabria, Johanna Walker, Holly Pham, Monica Ellwood-Lowe, Maria "Cat" Camacho, and Kira Oskirko for their assistance with data collection and organization. Finally, we thank the participants and their families participating in this study.

Author Contributions

I.H.G. designed research; D.M., S.M.C., and R.L.W. helped perform research; J.S.K. analyzed data; J.S.K., R.C., T.C.H., L.S.K. discussed results; J.S.K., R.C., T.C.H., L.S.K. A.J.G., and I.H.G. wrote paper.

References

Adrian, M., Miller, A. B., McCauley, E., & Stoep, A. V. (2016). Suicidal ideation in early to middle adolescence: Sex-specific trajectories and predictors. *Journal of Child Psychology and Psychiatry*, *57*(5), 645–653.

Andellini, M., Cannatà, V., Gazzellini, S., Bernardi, B., & Napolitano, A. (2015). Test-retest reliability of graph metrics of resting state MRI functional brain networks: A review. *Journal of Neuroscience Methods*, *253*, 183–192.

Auerbach, R. P., Pagliaccio, D., Allison, G. O., Alqueza, K. L., & Alonso, M. F. (2020). Neural Correlates Associated with Suicide and Non-Suicidal Self-Injury in Youth. *Biological Psychiatry*. Retrieved June 15, 2020, from http://www.sciencedirect.com/science/article/pii/S0006322320316711

Ballard, E. D., Lally, N., Nugent, A. C., Furey, M. L., Luckenbaugh, D. A., & Zarate, C. A. (2015). Neural Correlates of Suicidal Ideation and Its Reduction in Depression. *International Journal of Neuropsychopharmacology*, *18*(1), pyu069–pyu069.

Birn, R. M., Molloy, E. K., Patriat, R., Parker, T., Meier, T. B., Kirk, G. R., Nair, V. A., et al. (2013). The effect of scan length on the reliability of resting-state fMRI connectivity estimates. *NeuroImage*, *83*, 550–558.

Blomstedt, P., Hariz, M. I., Lees, A., Silberstein, P., Limousin, P., Yelnik, J., & Agid, Y. (2008). Acute severe depression induced by intraoperative stimulation of the substantia nigra: A case report. *Parkinsonism & Related Disorders*, *14*(3), 253–256.

Brent, D. A., Emslie, G. J., Clarke, G. N., Asarnow, J., Spirito, A., Ritz, L., Vitiello, B., et al. (2009). Predictors of spontaneous and systematically assessed suicidal adverse events in the

treatment of SSRI-resistant depression in adolescents (TORDIA) study. *The American Journal of Psychiatry*, *166*(4), 418–426.

Buuren, S. van, & Groothuis-Oudshoorn, K. (2011). mice: Multivariate Imputation by Chained Equations in R. *Journal of Statistical Software*, *45*(1), 1–67.

Bzdok, D., & Meyer-Lindenberg, A. (2018). Machine Learning for Precision Psychiatry: Opportunities and Challenges. *Biological Psychiatry: Cognitive Neuroscience and Neuroimaging*, *3*(3), 223–230.

Cao, J., Ai, M., Chen, X., Chen, J., Wang, W., & Kuang, L. (2020). Altered resting-state functional network connectivity is associated with suicide attempt in young depressed patients. *Psychiatry Research*, *285*, 112713.

Cha, C. B., Franz, P. J., Guzmán, E. M., Glenn, C. R., Kleiman, E. M., & Nock, M. K. (2018). Annual Research Review: Suicide among youth – epidemiology, (potential) etiology, and treatment. *Journal of Child Psychology and Psychiatry*, *59*(4), 460–482.

Coleman, L., & Coleman, J. (2002). The measurement of puberty: A review. *Journal of Adolescence*, *25*(5), 535–550.

Cox, ChristopherR., Moscardini, E. H., Cohen, A. S., & Tucker, R. P. (2020). Machine learning for suicidology: A practical review of exploratory and hypothesis-driven approaches. *Clinical Psychology Review*, 101940.

Earls, F. J., Brooks-Gunn, J., Raudenbush, S. W., & Sampson, R. J. (2007). Project on Human Development in Chicago Neighborhoods (PHDCN): Youth Self Report, Wave 1, 1994-1997. Inter-university Consortium for Political and Social Research [distributor].

Esteban, O., Markiewicz, C. J., Blair, R. W., Moodie, C. A., Isik, A. I., Erramuzpe, A., Kent, J. D., et al. (2019). fMRIPrep: A robust preprocessing pipeline for functional MRI. *Nature Methods*, *16*(1), 111–116. Nature Publishing Group.

Fan, L., Li, H., Zhuo, J., Zhang, Y., Wang, J., Chen, L., Yang, Z., et al. (2016). The Human Brainnetome Atlas: A New Brain Atlas Based on Connectional Architecture. *Cerebral Cortex (New York, NY)*, *26*(8), 3508–3526.

Fan, T., Wu, X., Yao, L., & Dong, J. (2013). Abnormal baseline brain activity in suicidal and non-suicidal patients with major depressive disorder. *Neuroscience Letters*, *534*, 35–40.

Franklin, J. C., Ribeiro, J. D., Fox, K. R., Bentley, K. H., Kleiman, E. M., Huang, X., Musacchio, K. M., et al. (2017). Risk factors for suicidal thoughts and behaviors: A meta-analysis of 50 years of research. *Psychological Bulletin*, *143*(2), 187–232.

Friedman, J., Hastie, T., & Tibshirani, R. (2010). Regularization Paths for Generalized Linear Models via Coordinate Descent. *Journal of Statistical Software*, *33*(1). Retrieved May 26, 2020, from http://www.jstatsoft.org/v33/i01/

Gabbay, V., Liu, Q., DeWitt, S. J., Mehra, L. M., Alonso, C. M., & Ely, B. A. (2020). Neural Correlates of Positive and Negative Valence System Dysfunction in Adolescents Revealed by Data-Driven Parcellation and Resting-State Network Modeling. *BioRxiv*, 2020.03.20.001032. Cold Spring Harbor Laboratory.

Gifuni, A. J., Perret, L. C., Lacourse, E., Geoffroy, M.-C., Mbekou, V., Jollant, F., & Renaud, J. (2020). Decision-making and cognitive control in adolescent suicidal behaviors: A qualitative systematic review of the literature. *European Child & Adolescent Psychiatry*. Retrieved May 25, 2020, from http://link.springer.com/10.1007/s00787-020-01550-3

Gorgolewski, K., Burns, C. D., Madison, C., Clark, D., Halchenko, Y. O., Waskom, M. L., & Ghosh, S. S. (2011). Nipype: A Flexible, Lightweight and Extensible Neuroimaging Data Processing Framework in Python. *Frontiers in Neuroinformatics*, *5*. Frontiers. Retrieved April 21, 2020, from https://www.frontiersin.org/articles/10.3389/fninf.2011.00013/full

Gorgolewski, K. J., Esteban, O., Ellis, D. G., Notter, M. P., Ziegler, E., Johnson, H., Hamalainen, C., et al. (2017). *Nipype: A flexible, lightweight and extensible neuroimaging data processing framework in Python. 0.13.1*. Zenodo. Retrieved April 29, 2020, from https://zenodo.org/record/581704#.XqpcY1NKiqA

Grayson, D. S., & Fair, D. A. (2017). Development of large-scale functional networks from birth to adulthood: A guide to the neuroimaging literature. *NeuroImage*, *160*, 15–31.

Hallquist, M. N., & Hillary, F. G. (2018). Graph theory approaches to functional network organization in brain disorders: A critique for a brave new small-world. *Network Neuroscience*, *3*(1), 1–26.

Hawton, K., Saunders, K. E., & O'Connor, R. C. (2012). Self-harm and suicide in adolescents. *The Lancet*, *379*(9834), 2373–2382.

van Heeringen, K., Wu, G.-R., Vervaet, M., Vanderhasselt, M.-A., & Baeken, C. (2017). Decreased resting state metabolic activity in frontopolar and parietal brain regions is associated with suicide plans in depressed individuals. *Journal of Psychiatric Research*, *84*, 243–248.

van den Heuvel, M. P., de Lange, S. C., Zalesky, A., Seguin, C., Yeo, B. T. T., & Schmidt, R. (2017). Proportional thresholding in resting-state fMRI functional connectivity networks and consequences for patient-control connectome studies: Issues and recommendations. *NeuroImage*, *152*, 437–449.

Ho, T. C., King, L. S., Leong, J. K., Colich, N. L., Humphreys, K. L., Ordaz, S. J., & Gotlib, I. H. (2017). Effects of sensitivity to life stress on uncinate fasciculus segments in early adolescence. *Social Cognitive and Affective Neuroscience*, *12*(9), 1460–1469.

Holmes, S. E., Hinz, R., Conen, S., Gregory, C. J., Matthews, J. C., Anton-Rodriguez, J. M., Gerhard, A., et al. (2018). Elevated Translocator Protein in Anterior Cingulate in Major Depression and a Role for Inflammation in Suicidal Thinking: A Positron Emission Tomography Study. *Biological Psychiatry*, *83*(1), 61–69.

Hosseini, S. M. H., Hoeft, F., & Kesler, S. R. (2012). GAT: A Graph-Theoretical Analysis Toolbox for Analyzing Between-Group Differences in Large-Scale Structural and Functional Brain Networks. *PLoS ONE*, *7*(7). Retrieved May 12, 2020, from https://www.ncbi.nlm.nih.gov/pmc/articles/PMC3396592/

James, G., Witten, D., Hastie, T., & Tibshirani, R. (2013). Resampling Methods. In G. James, D. Witten, T. Hastie, & R. Tibshirani (Eds.), *An Introduction to Statistical Learning: With Applications in R*, Springer Texts in Statistics (pp. 175–201). New York, NY: Springer. Retrieved November 11, 2020, from https://doi.org/10.1007/978-1-4614-7138-7_5

Jung, J., Choi, S., Han, K.-M., Kim, A., Kang, W., Paik, J.-W., Lee, H.-W., et al. (2020). Alterations in functional brain networks in depressed patients with a suicide attempt history. *Neuropsychopharmacology*, *45*(6), 964–974. Nature Publishing Group.

Kang, S.-G., Na, K.-S., Choi, J.-W., Kim, J.-H., Son, Y.-D., & Lee, Y. J. (2017). Resting-state functional connectivity of the amygdala in suicide attempters with major depressive disorder. *Progress in Neuro-Psychopharmacology and Biological Psychiatry*, *77*, 222–227.

Kaufman, J., Birmaher, B., Brent, D., Rao, U., Flynn, C., Moreci, P., Williamson, D., et al. (1997). Schedule for Affective Disorders and Schizophrenia for School-Age Children-Present and Lifetime Version (K-SADS-PL): Initial reliability and validity data. *Journal of the American Academy of Child and Adolescent Psychiatry*, *36*(7), 980–988.

Keuken, M. C., & Forstmann, B. U. (2015). A probabilistic atlas of the basal ganglia using 7 T MRI. *Data in Brief*, *4*, 577–582.

Kim, K., Kim, S.-W., Myung, W., Han, C. E., Fava, M., Mischoulon, D., Papakostas, G. I., et al. (2017). Reduced orbitofrontal-thalamic functional connectivity related to suicidal ideation in patients with major depressive disorder. *Scientific Reports*, *7*(1), 1–11. Nature Publishing Group.

King, C. A., Brent, D., Grupp-Phelan, J., Shenoi, R., Page, K., Mahabee-Gittens, E. M., Chernick, L. S., et al. (2019). Five Profiles of Adolescents at Elevated Risk for Suicide Attempts: Differences in Mental Health Service Use. *Journal of the American Academy of Child & Adolescent Psychiatry*, S0890856719322221.

King, L. S., Colich, N. L., LeMoult, J., Humphreys, K. L., Ordaz, S. J., Price, A. N., & Gotlib, I. H. (2017). The impact of the severity of early life stress on diurnal cortisol: The role of puberty. *Psychoneuroendocrinology*, *77*, 68–74.

King, L. S., Graber, M. G., Colich, N. L., & Gotlib, I. H. (2020). Associations of waking cortisol with DHEA and testosterone across the pubertal transition: Effects of threat-related early life stress. *Psychoneuroendocrinology*, *115*, 104651.

King, L. S., Humphreys, K. L., Camacho, M. C., & Gotlib, I. H. (2019). A person-centered approach to the assessment of early life stress: Associations with the volume of stress-sensitive brain regions in early adolescence. *Development and Psychopathology*, *31*(02), 643–655.

Klonsky, E. D., May, A. M., & Saffer, B. Y. (2016). Suicide, Suicide Attempts, and Suicidal Ideation. *Annual Review of Clinical Psychology*, *12*(1), 307–330.

Kruschwitz, J. D., List, D., Waller, L., Rubinov, M., & Walter, H. (2015). GraphVar: A user-friendly toolbox for comprehensive graph analyses of functional brain connectivity. *Journal of Neuroscience Methods*, *245*, 107–115.

LaVome Robinson, W., Droege, J. R., Hipwell, A. E., Stepp, S. D., & Keenan, K. (2016). Brief report: Suicidal ideation in adolescent girls: Impact of race. *Journal of Adolescence*, *53*, 16–20.

Lydon-Staley, D. M., Ciric, R., Satterthwaite, T. D., & Bassett, D. S. (2018). Evaluation of confound regression strategies for the mitigation of micromovement artifact in studies of dynamic resting-state functional connectivity and multilayer network modularity. *Network Neuroscience*, *3*(2), 427–454. MIT Press.

Marshall, W. A., & Tanner, J. M. (1969). Variations in pattern of pubertal changes in girls. *Archives of Disease in Childhood*, *44*(235), 291–303.

Marshall, W. A., & Tanner, J. M. (1970). Variations in the Pattern of Pubertal Changes in Boys. *Archives of Disease in Childhood*, *45*(239), 13–23.

Matthews, M., & Fair, D. A. (2015). Research Review: Functional brain connectivity and child psychopathology – overview and methodological considerations for investigators new to the field. *Journal of Child Psychology and Psychiatry*, *56*(4), 400–414.

Menon, V. (2011). Large-scale brain networks and psychopathology: A unifying triple network model. *Trends in Cognitive Sciences*, *15*(10), 483–506.

Morris, N. M., & Udry, J. R. (1980). Validation of a self-administered instrument to assess stage of adolescent development. *Journal of youth and adolescence*, *9*(3), 271–280. United States.

National Center for Health Statistics (NCHS), National Vital Statistics System, National Center for Injury Prevention and Control, Centers for Disease Control and Prevention, & National Institute of Mental Health (NIMH). (2017). *Centers for Disease Control and Prevention (CDC) WISQARS Leading Causes of Death Reports, in 2017*. Retrieved May 27, 2020, from https://www.nimh.nih.gov/health/statistics/suicide.shtml

Nock, M. K., Green, J. G., Hwang, I., McLaughlin, K. A., Sampson, N. A., Zaslavsky, A. M., & Kessler, R. C. (2013). Prevalence, Correlates, and Treatment of Lifetime Suicidal Behavior Among Adolescents: Results From the National Comorbidity Survey Replication Adolescent Supplement. *JAMA Psychiatry*, *70*(3), 300.

Ordaz, S. J., Goyer, M. S., Ho, T. C., Singh, M. K., & Gotlib, I. H. (2018). Network basis of suicidal ideation in depressed adolescents. *Journal of Affective Disorders*, *226*, 92–99.

Pan, L. A., Hassel, S., Segreti, A. M., Nau, S. A., Brent, D. A., & Phillips, M. L. (2013). Differential patterns of activity and functional connectivity in emotion processing neural circuitry to angry and happy faces in adolescents with and without suicide attempt. *Psychological Medicine*, *43*(10), 2129–2142.

Pan, Lisa A., Batezati-Alves, S. C., Almeida, J. R. C., Segreti, A., Akkal, D., Hassel, S., Lakdawala, S., et al. (2011). Dissociable Patterns of Neural Activity During Response Inhibition in

Depressed Adolescents With and Without Suicidal Behavior. *Journal of the American Academy of Child & Adolescent Psychiatry*, *50*(6), 602-611.e3.

Prinstein, M. J., Nock, M. K., Simon, V., Aikins, J. W., Cheah, C. S. L., & Spirito, A. (2008). Longitudinal trajectories and predictors of adolescent suicidal ideation and attempts following inpatient hospitalization. *Journal of Consulting and Clinical Psychology*, *76*(1), 92–103.

R Core Team. (2019). *R: A Language and Environment for Statistical Computing*. Vienna, Austria: R Foundation for Statistical Computing. Retrieved from https://www.R-project.org/

Reynolds, W. M. (1988). Suicidal Ideation Questionnaire—Junior. *Psychological Assessment Resources, Odessa, FL*.

Ribbe, D. (1996). Psychometric review of Traumatic Events Screening Inventory for Children (TESI-C). *In B. H. Stamm (Ed.),Measurement of stress, trauma, and adaptation. Lutherville, MD: Sidran*, 386–387.

Richter, A., Reinhard, F., Kraemer, B., & Gruber, O. (2020). A high-resolution fMRI approach to characterize functionally distinct neural pathways within dopaminergic midbrain and nucleus accumbens during reward and salience processing. *European Neuropsychopharmacology*, *36*, 137–150.

Rubinov, M., & Sporns, O. (2010). Complex network measures of brain connectivity: Uses and interpretations. *NeuroImage*, *52*(3), 1059–1069.

Ruch, D. A., Sheftall, A. H., Schlagbaum, P., Rausch, J., Campo, J. V., & Bridge, J. A. (2019). Trends in Suicide Among Youth Aged 10 to 19 Years in the United States, 1975 to 2016. *JAMA Network Open*, *2*(5), e193886–e193886. American Medical Association.

Ruderfer, D. M., Walsh, C. G., Aguirre, M. W., Tanigawa, Y., Ribeiro, J. D., Franklin, J. C., & Rivas, M. A. (2019). Significant shared heritability underlies suicide attempt and clinically predicted probability of attempting suicide. *Molecular Psychiatry*, 1–9. Nature Publishing Group.

Schmaal, L., van Harmelen, A.-L., Chatzi, V., Lippard, E. T. C., Toenders, Y. J., Averill, L. A., Mazure, C. M., et al. (2020). Imaging suicidal thoughts and behaviors: A comprehensive review of 2 decades of neuroimaging studies. *Molecular Psychiatry*, *25*(2), 408–427. Nature Publishing Group.

Schreiner, M. W., Klimes-Dougan, B., & Cullen, K. R. (2019). Neural Correlates of Suicidality in Adolescents with Major Depression: Resting-State Functional Connectivity of the Precuneus and Posterior Cingulate Cortex. *Suicide and Life-Threatening Behavior*, *49*(3), 899–913.

Schwartz, J., Ordaz, S. J., Ho, T. C., & Gotlib, I. H. (2019). Longitudinal decreases in suicidal ideation are associated with increases in salience network coherence in depressed adolescents. *Journal of Affective Disorders*, *245*, 545–552.

Seeley, W. W., Menon, V., Schatzberg, A. F., Keller, J., Glover, G. H., Kenna, H., Reiss, A. L., et al. (2007). Dissociable Intrinsic Connectivity Networks for Salience Processing and Executive Control. *Journal of Neuroscience*, *27*(9), 2349–2356.

Shirtcliff, E. A., Dahl, R. E., & Pollak, S. D. (2009). Pubertal Development: Correspondence Between Hormonal and Physical Development: Hormonal Correlates of Pubertal Stage. *Child Development*, *80*(2), 327–337.

Sporns, O. (2018). Graph theory methods: Applications in brain networks. *Dialogues in Clinical Neuroscience*, *20*(2), 111–121.

Stewart, J. G., Shields, G. S., Esposito, E. C., Cosby, E. A., Allen, N. B., Slavich, G. M., & Auerbach, R. P. (2019). Life Stress and Suicide in Adolescents. *Journal of Abnormal Child Psychology*, *47*(10), 1707–1722.

Sublette, M. E., Milak, M. S., Galfalvy, H. C., Oquendo, M. A., Malone, K. M., & Mann, J. J. (2013). Regional Brain Glucose Uptake Distinguishes Suicide Attempters from Non-Attempters in Major Depression. *Archives of Suicide Research*, *17*(4), 434–447. Routledge.

Termenon, M., Jaillard, A., Delon-Martin, C., & Achard, S. (2016). Reliability of graph analysis of resting state fMRI using test-retest dataset from the Human Connectome Project. *NeuroImage*, *142*, 172–187.

Tibshirani, R. (1996). Regression Shrinkage and Selection Via the Lasso. *Journal of the Royal Statistical Society: Series B (Methodological)*, *58*(1), 267–288.

Uddin, L. Q. (2015). Salience processing and insular cortical function and dysfunction. *Nature Reviews Neuroscience*, *16*(1), 55–61.

Utter, A. A., & Basso, M. A. (2008). The basal ganglia: An overview of circuits and function. *Neuroscience & Biobehavioral Reviews*, *32*(3), 333–342.

Van Dijk, K. R. A., Hedden, T., Venkataraman, A., Evans, K. C., Lazar, S. W., & Buckner, R. L. (2010). Intrinsic functional connectivity as a tool for human connectomics: Theory, properties, and optimization. *Journal of Neurophysiology*, *103*(1), 297–321.

Wagner, G., de la Cruz, F., Köhler, S., Pereira, F., Richard-Devantoy, S., Turecki, G., Bär, K.-J., et al. (2019). Connectomics-Based Functional Network Alterations in both Depressed Patients with Suicidal Behavior and Healthy Relatives of Suicide Victims. *Scientific Reports*, *9*(1), 14330.

Weng, J.-C., Chou, Y.-S., Tsai, Y.-H., Lee, C.-T., Hsieh, M.-H., & Chen, V. C.-H. (2019). Connectome Analysis of Brain Functional Network Alterations in Depressive Patients with Suicidal Attempt. *Journal of Clinical Medicine*, *8*(11). Retrieved March 3, 2020, from https://www.ncbi.nlm.nih.gov/pmc/articles/PMC6912611/

Whalen, D. J., Luby, J. L., & Barch, D. M. (2018). Highlighting risk of suicide from a developmental perspective. *Clinical Psychology: Science and Practice*, *25*(1), e12229.

Zhang, X., Braun, U., Tost, H., & Bassett, D. S. (2020). Data-Driven Approaches to Neuroimaging Analysis to Enhance Psychiatric Diagnosis and Therapy. *Biological Psychiatry: Cognitive Neuroscience and Neuroimaging*. Retrieved April 29, 2020, from http://www.sciencedirect.com/science/article/pii/S2451902219303556

Zou, H., & Hastie, T. (2005). Regularization and variable selection via the elastic net. *Journal of the Royal Statistical Society: Series B (Statistical Methodology)*, *67*(2), 301–320.

Supplemental Information

Early Life Stress Interview

For each type of stress that the participant endorsed, interviewers followed up with specific questions to characterize the severity of the stressful experience. As described in King et al. (2017, 2019), a panel of three coders, blind to the children's subjective severity ratings and reactions and behaviors during the interview, then rated the objective severity of each type of stressor endorsed using a modified version of the UCLA Life Stress Interview coding system (Rudolph et al., 2000). Coders made objective severity ratings on a 5-point scale with an ICC of 0.99 (King et al., 2017).

fMRI Preprocessing

Anatomical data preprocessing

The T1-weighted (T1w) image was corrected for intensity non-uniformity (INU) with N4BiasFieldCorrection (Tustison et al., 2010), distributed with ANTs 2.2.0 (Avants et al., 2008), RRID:SCR_004757, and used as T1w-reference throughout the workflow.

The T1w-reference was then skull-stripped with a *Nipype* implementation of the antsBrainExtraction.sh workflow (from ANTs), using OASIS30ANTs as target template. Brain tissue segmentation of cerebrospinal fluid (CSF), white-matter (WM) and gray-matter (GM) was performed on the brain-extracted T1w using fast (FSL 5.0.9, RRID:SCR_002823) (Zhang et al., 2001). Brain surfaces were reconstructed using recon-all (FreeSurfer 6.0.1, RRID:SCR_001847) (Dale et al., 1999), and the brain mask estimated previously was refined with a custom variation of the method to reconcile ANTs-derived and FreeSurfer-derived segmentations of the cortical gray-matter of Mindboggle (RRID:SCR_002438) (Klein et al., 2017). Volume-based spatial normalization to standard space (*MNI's unbiased standard MRI template for pediatric data from the 4.5 to 18.5y age range* [RRID:SCR_008796; TemplateFlow ID: MNIPediatricAsym) was performed through nonlinear registration

with antsRegistration (ANTs 2.2.0), using brain-extracted versions of both T1w reference and the T1w template.

Functional data preprocessing

First, a reference volume and its skull-stripped version were generated using a custom methodology of *fMRIPrep*. Based on the estimated susceptibility distortion, an unwarped BOLD reference was calculated for a more accurate co-registration with the anatomical reference. The BOLD reference was then co-registered to the T1w reference using bbregister (FreeSurfer) which implements boundary-based registration (Greve & Fischl, 2009). Co-registration was configured with six degrees of freedom. Head-motion parameters with respect to the BOLD reference (transformation matrices, and six corresponding rotation and translation parameters) are estimated before any spatiotemporal filtering using mcflirt (FSL 5.0.9) (Jenkinson et al., 2002). BOLD runs were slice-time corrected using 3dTshift from AFNI 20160207 (RRID:SCR_005927) (Cox & Hyde, 1997). The BOLD time-series, were resampled to surfaces on the following spaces: *fsaverage5*. The BOLD time-series (including slice-timing correction when applied) were resampled onto their original, native space by applying a single, composite transform to correct for head-motion and susceptibility distortions. These resampled BOLD time-series will be referred to as *preprocessed BOLD in original space*, or just *preprocessed BOLD*. The BOLD time-series were resampled into standard space (MNIPediatricAsym), correspondingly generating the following *spatially-normalized, preprocessed BOLD runs*. First, a reference volume and its skull-stripped version were generated using a custom methodology of *fMRIPrep*. Several confounding time-series were calculated based on the *preprocessed BOLD*: framewise displacement (FD), DVARS and three region-wise global signals. FD and DVARS are calculated for each functional run, both using their implementations in *Nipype* (following the definitions by Power et al. 2014) (Power et al., 2014). The three global signals are extracted within the CSF, the WM, and the whole-brain masks. Additionally, a set of physiological regressors were extracted to allow for component-based noise correction,

CompCor (Behzadi et al., 2007). Principal components are estimated after high-pass filtering the *preprocessed BOLD* time-series (using a discrete cosine filter with 128s cut-off) for the two *CompCor* variants: temporal (tCompCor) and anatomical (aCompCor). tCompCor components are then calculated from the top 5% variable voxels within a mask covering the subcortical regions. This subcortical mask is obtained by heavily eroding the brain mask, which ensures it does not include cortical GM regions. For aCompCor, components are calculated within the intersection of the aforementioned mask and the union of CSF and WM masks calculated in T1w space, after their projection to the native space of each functional run (using the inverse BOLD-to-T1w transformation). Components are also calculated separately within the WM and CSF masks. For each CompCor decomposition, the *k* components with the largest singular values are retained, such that the retained components' time series are sufficient to explain 50 percent of variance across the nuisance mask (CSF, WM, combined, or temporal). The remaining components are dropped from consideration. The head-motion estimates calculated in the correction step were also placed within the corresponding confounds file. The confound time series derived from head motion estimates and global signals were expanded with the inclusion of temporal derivatives and quadratic terms for each (Satterthwaite et al., 2013). Frames that exceeded a threshold of 0.5 mm FD or 1.5 standardised DVARS were annotated as motion outliers. All resamplings can be performed with *a single interpolation step* by composing all the pertinent transformations (i.e. head-motion transform matrices, susceptibility distortion correction when available, and co-registrations to anatomical and output spaces). Gridded (volumetric) resamplings were performed using antsApplyTransforms (ANTs), configured with Lanczos interpolation to minimize the smoothing effects of other kernels (Lanczos, 1964). Non-gridded (surface) resamplings were performed using mri_vol2surf (FreeSurfer).

Following preprocessing in fMRIPrep, the first 6 frames were discarded to allow the MR signal to achieve T1 equilibrium. We then conducted nuisance regression (nuisance regressors

included framewise displacement, translation and rotation, and their first and second derivatives, and aCompCor components 0-5) followed by temporal band-pass filtering (.01 - .1 Hz) to the resting-state data. Post-processing steps included intensity normalization of the time series, and motion-censoring (using interpolation) for frames that exceed 0.5mm FD. We also included a supplemental analysis assessing the correlation between FD and the variables with non-zero estimates from the LASSO regression. This analysis revealed only one significant correlation between degree of the left intermediate lateral inferior temporal gyrus and mean framewise displacement (β =-.27, *p*=.034, corrected). We therefore tested whether degree of the left intermediate lateral inferior temporal gyrus was associated with future severity of SI above and beyond mean framewise displacement. This analysis revealed that degree of the left intermediate lateral inferior temporal gyrus was associated with future severity of SI (β=.20, *p*=.042) above and beyond mean framewise displacement (β=.07, *p*=.721).

Supplemental Analysis of Non-Graph theory brain-based Baseline Variables

We conducted separate linear regressions for each non-brain baseline variable (sex, pubertal stage, race, age, BMI, internalizing symptom severity, the interval between the time points, objective ELS severity, subjective ELS sensitivity, SES, mean framewise displacement, sleepiness during scan) to determine if any predicted severity of SI. We also modeled the interaction of Tanner score and sex to examine whether sex moderated the effect of Tanner on the severity of SI. Only the main effect of sex was moderate (β = .43, *p*=.029, uncorrected). Framewise displacement, age, ELS sensitivity, and parent education level were not significantly associated with future severity of SI (see *Supplemental Table 3*). Some research has reported that sex differences are more common in self-harming behaviors than in SI (Hawton et al., 2012; Oquendo et al., 2007). In contrast, however, there are also robust findings of a higher prevalence of ideation and attempts in girls than in boys (Fox et al., 2018). Although pubertal timing (i.e., the age of pubertal onset) has been found to predict severity of SI (Patton & Viner,

2007), because girls and boys in our sample were matched on pubertal status and not on age, we cannot estimate the onset of puberty in our participants. It is well recognized that exposure to stressful life events is a potent risk factor for the development of suicidal thoughts and behaviors in adolescents (Dykxhoorn et al., 2017; Miller & Prinstein, 2019). It is possible that our sample on average did not experience high enough levels of stress to detect an effect. Delineating which aspects of adversity predict severity of SI can help to target interventions. As expected, baseline internalizing severity, a known risk factor for suicidal thoughts and behaviors, predicted severity of SI in our sample in our LASSO and OLS regression. Sex did not appear as a predictor in our LASSO analysis, possibly due to the penalization level. However, sex was a predictor in the LASSO regression of internalizing symptom severity. Since our instructions for the scan was to keep eyes closed, but remain awake, it is possible that sleepiness could occur. At the end of the scan, participants self-report whether they experienced sleepiness during the scan. Most participants (N=71) experienced some feelings of sleepiness during the scan. We thus, examined sleepiness as a binary dummy coded variable in relation to severity of SI. There was no significant association between whether participants experienced sleepiness during the scan and severity of SI (see *Supplementary Table 3*).

Supplemental Table 1. Medications at Baseline

Type	Generic (Brand)	N
Antihistamine	Lortadine (Claritin), Cetirizine (Zyrtec), Fexofenadine (Allegra), un-named allergy medication	6
Anti-inflammatory	Montelukast (Singulair)	1
Steroid or Corticosteroid	Fluticasone Propionate (Flonase), formoterole and mometasone (Dulera)	3
Bronchodilator	Albuterol (Inhaler), inhaler	2
Stimulants	Methylphenidate (Concerta, Ritalin), Dexmethylphenidate (Focalin)	7
Sedative	Clonidine	1
Antihistamine and Antacid	Famotidine (Pepcid)	1
Laxative	Polyethylene Glycol 3350 (Miralax)	1
Supplements	Probiotics, Vitamins, Melatonin	3

Supplemental Table 2. Measures with Missing Observations

Measure	Number of Missing Observations
YSR-baseline	2
YSR-follow-up	6
ELS stress sensitivity	3
Parent Education	6
BMI baseline	3
Tanner follow-up	5

YSR = Youth Self Report; ELS = Early Life Stress. Missing values were imputed using Multivariate Imputation by Chained Equations

Supplemental Table 3. Results of baseline covariates in relation to SI.

Variable	Estimate (β)	*p*-value uncorrected	*p*-value corrected (FDR)
Sex	0.43	**0.026**	0.1320
Race (0=White, 1=POC)	-0.07	0.726	0.8256
Age baseline (years)	-0.20	**0.040**	0.1320
Tanner at baseline	0.03	0.743	0.8256
Internalizing severity at baseline	0.18	0.059	0.1480
Interval between baseline and later assessment (years)	0.20	**0.035**	0.1320
ELS (objective severity)	0.16	0.094	0.1874
ELS (sensitivity)	0.04	0.675	0.8256
Parent Education	0.13	0.184	0.3067
BMI	0.00	1.000	1.0000
Mean FD	0.02	0.869	0.8691
any sleepiness during scan	0.34	0.099	0.1810

Note. POC = people of color; ELS = early life stress; YSR = Youth Self Report; FD = Framewise Displacement; sleepiness during scan indicates if there was any self-reported sleepiness during the entirety of the scan. p-values < .05 are bolded.

Supplemental Table 4. Correlations between Framewise displacement and LASSO-based predictors of severity of suicidal ideation

Variable	Estimate (β)	*p*-value uncorrected	*p*-value corrected (FDR)
Internalizing severity at baseline	-0.04	0.671	0.856
caudIFG (R) Degree	0.11	0.246	0.656
caudvlPrG (L) Degree	0.15	0.123	0.492
SN (R) Within-module degree	-0.02	0.856	0.856
medventFuG (L) Degree	-0.03	0.787	0.856
intlatITG (L) Degree	**-0.27**	**0.004**	**0.034**
sgCG (R) Eigenvector Centrality	-0.08	0.426	0.852
rostdorIPL (R) Within-module degree	-0.02	0.855	0.856

Note. p-values < .05 are bolded. L = Left; R = Right; FDR = False Discovery Rate; caudIFG = caudal inferior frontal gyrus; caudvlPrG = caudal ventrolateral precentral gyrus; SN = substantia nigra; medventFuG = medioventral fusiform gyrus; intlatITG = intermediate lateral inferior temporal gyrus; sgCG = subgenual cingulate gyrus; rostdorIPL = rostrodorsal inferior parietal lobe

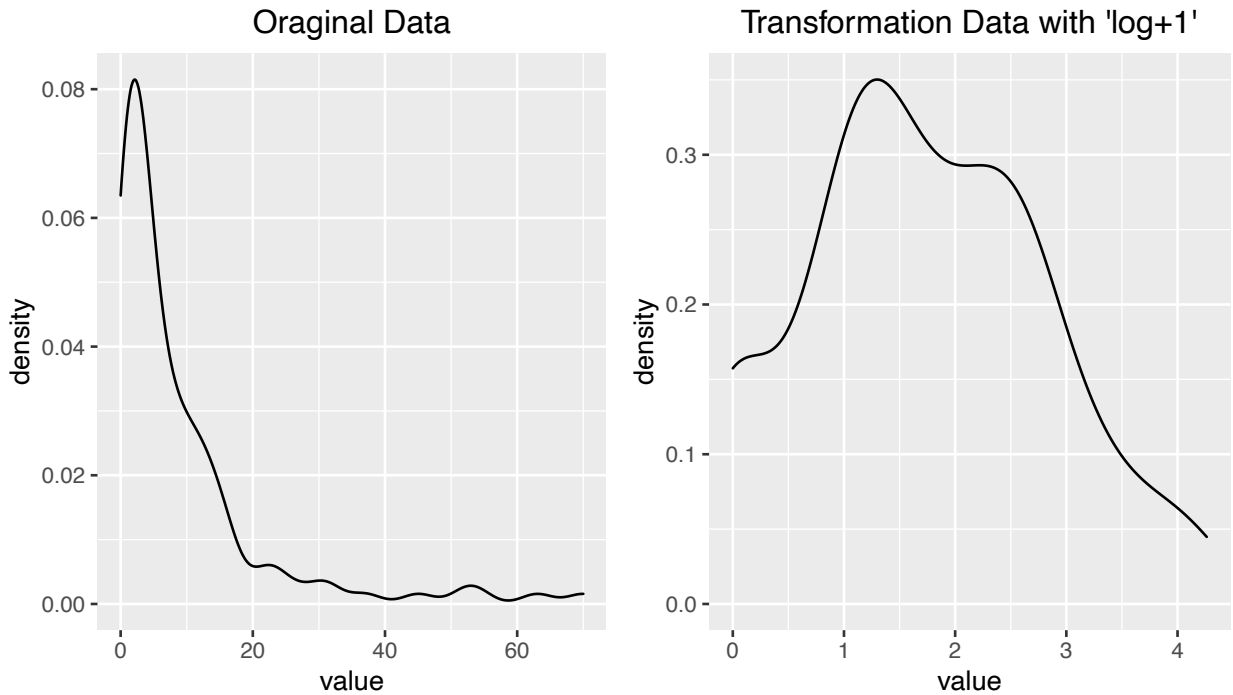

Supplemental Figure 1. Log-transformation of suicidal ideation severity scores (N = 109). 1 was added to scores given some values were zero.

References

Avants, B. B., Epstein, C. L., Grossman, M., & Gee, J. C. (2008). Symmetric diffeomorphic image registration with cross-correlation: Evaluating automated labeling of elderly and neurodegenerative brain. *Medical Image Analysis*, *12*(1), 26–41. https://doi.org/10.1016/j.media.2007.06.004

Behzadi, Y., Restom, K., Liau, J., & Liu, T. T. (2007). A component based noise correction method (CompCor) for BOLD and perfusion based fMRI. *NeuroImage*, *37*(1), 90–101. https://doi.org/10.1016/j.neuroimage.2007.04.042

Cox, R. W., & Hyde, J. S. (1997). Software tools for analysis and visualization of fMRI data. *NMR in Biomedicine*, *10*(4–5), 171–178. https://doi.org/10.1002/(sici)1099-1492(199706/08)10:4/5<171::aid-nbm453>3.0.co;2-l

Dale, A. M., Fischl, B., & Sereno, M. I. (1999). Cortical Surface-Based Analysis: I. Segmentation and Surface Reconstruction. *NeuroImage*, *9*(2), 179–194. https://doi.org/10.1006/nimg.1998.0395

Dykxhoorn, J., Hatcher, S., Roy-Gagnon, M.-H., & Colman, I. (2017). Early life predictors of adolescent suicidal thoughts and adverse outcomes in two population-based cohort studies. *PLOS ONE*, *12*(8), e0183182. https://doi.org/10.1371/journal.pone.0183182

Fox, K. R., Millner, A. J., Mukerji, C. E., & Nock, M. K. (2018). Examining the role of sex in self-injurious thoughts and behaviors. *Clinical Psychology Review*, *66*, 3–11. https://doi.org/10.1016/j.cpr.2017.09.009

Greve, D. N., & Fischl, B. (2009). Accurate and robust brain image alignment using boundary-based registration. *NeuroImage*, *48*(1), 63–72. https://doi.org/10.1016/j.neuroimage.2009.06.060

Hawton, K., Saunders, K. E., & O'Connor, R. C. (2012). Self-harm and suicide in adolescents. *The Lancet*, *379*(9834), 2373–2382. https://doi.org/10.1016/S0140-6736(12)60322-5

Jenkinson, M., Bannister, P., Brady, M., & Smith, S. (2002). Improved optimization for the robust and accurate linear registration and motion correction of brain images. *NeuroImage*, *17*(2), 825–841. https://doi.org/10.1016/s1053-8119(02)91132-8

King, L. S., Colich, N. L., LeMoult, J., Humphreys, K. L., Ordaz, S. J., Price, A. N., & Gotlib, I. H. (2017). The impact of the severity of early life stress on diurnal cortisol: The role of puberty. *Psychoneuroendocrinology*, *77*, 68–74. https://doi.org/10.1016/j.psyneuen.2016.11.024

King, L. S., Humphreys, K. L., Camacho, M. C., & Gotlib, I. H. (2019). A person-centered approach to the assessment of early life stress: Associations with the volume of stress-sensitive brain regions in early adolescence. *Development and Psychopathology*, *31*(02), 643–655. https://doi.org/10.1017/S0954579418000184

Klein, A., Ghosh, S. S., Bao, F. S., Giard, J., Häme, Y., Stavsky, E., Lee, N., Rossa, B., Reuter, M., Neto, E. C., & Keshavan, A. (2017). Mindboggling morphometry of human brains. *PLOS Computational Biology*, *13*(2), e1005350. https://doi.org/10.1371/journal.pcbi.1005350

Lanczos, C. (1964). Evaluation of Noisy Data. *Journal of the Society for Industrial and Applied Mathematics Series B Numerical Analysis*, *1*(1), 76–85. https://doi.org/10.1137/0701007

Miller, A. B., & Prinstein, M. J. (2019). Adolescent Suicide as a Failure of Acute Stress-Response Systems. *Annual Review of Clinical Psychology*, *15*(1), 425–450. https://doi.org/10.1146/annurev-clinpsy-050718-095625

Oquendo, M. A., Bongiovi-Garcia, M. E., Galfalvy, H., Goldberg, P. H., Grunebaum, M. F., Burke, A. K., & Mann, J. J. (2007). Sex Differences in Clinical Predictors of Suicidal Acts After Major Depression: A Prospective Study. *American Journal of Psychiatry*, *164*(1), 134–141. https://doi.org/10.1176/ajp.2007.164.1.134

Patton, G. C., & Viner, R. (2007). Pubertal transitions in health. *The Lancet*, *369*(9567), 1130–1139. https://doi.org/10.1016/S0140-6736(07)60366-3

Power, J. D., Mitra, A., Laumann, T. O., Snyder, A. Z., Schlaggar, B. L., & Petersen, S. E. (2014). Methods to detect, characterize, and remove motion artifact in resting state fMRI. *NeuroImage*, *84*. https://doi.org/10.1016/j.neuroimage.2013.08.048

Rudolph, K. D., Hammen, C., Burge, D., Lindberg, N., Herzberg, D., & Daley, S. E. (2000). Toward an interpersonal life-stress model of depression: The developmentalcontext of stress generation. *Developmental Psychopathology*, *12*, 215–234.

Satterthwaite, T. D., Elliott, M. A., Gerraty, R. T., Ruparel, K., Loughead, J., Calkins, M. E., Eickhoff, S. B., Hakonarson, H., Gur, R. C., Gur, R. E., & Wolf, D. H. (2013). An improved framework for confound regression and filtering for control of motion artifact in the preprocessing of resting-state functional connectivity data. *NeuroImage*, *64*, 240–256. https://doi.org/10.1016/j.neuroimage.2012.08.052

Tustison, N. J., Avants, B. B., Cook, P. A., Zheng, Y., Egan, A., Yushkevich, P. A., & Gee, J. C. (2010). N4ITK: Improved N3 Bias Correction. *IEEE Transactions on Medical Imaging*, *29*(6), 1310–1320. https://doi.org/10.1109/TMI.2010.2046908

Zhang, Y., Brady, M., & Smith, S. (2001). Segmentation of brain MR images through a hidden Markov random field model and the expectation-maximization algorithm. *IEEE Transactions on Medical Imaging*, *20*(1), 45–57. https://doi.org/10.1109/42.906424